

1 **Lithospheric deformation in the Canadian Appalachians:**
2 **evidence from shear wave splitting**

3

4 Amy Gilligan (1), Ian D. Bastow (1), Emma Watson (1), Fiona A. Darbyshire (2),
5 Vadim Levin (3), William Menke (4), Victoria Lane (5) David Hawthorn (5),(6)
6 Alistair Boyce (1) Mitchell V. Liddell (1) Laura Petrescu (1)

7

8 (1) Department of Earth Science and Engineering, Imperial College London,
9 London, UK, SW7 2AZ

10 (2) GEOTOP, Université du Québec à Montréal, Montréal, Québec, Canada

11 (3) Department of Earth and Planetary Sciences, Rutgers University,
12 Piscataway, NJ, USA

13 (4) Lamont-Doherty Earth Observatory, Columbia University, Palisades, NY,
14 USA

15 (5) SEIS-UK, University of Leicester, Leicester, UK, LE1 7RH

16 (6) BGS Murchison House, W Mains Rd, Edinburgh, UK, EH9 3LA

17

18 Accepted: 27th May 2016 Received: 27th May 2016; in original form: 11th January
19 2016

20

21 Short title: Lithospheric deformation in the Canadian Appalachians

22

23 Corresponding author: Amy Gilligan, a.gilligan@imperial.ac.uk

24

25

26 **Summary**

27

28 Plate-scale deformation is expected to impart seismic anisotropic fabrics on the
29 lithosphere. Determination of the fast shear wave orientation (ϕ) and the delay-
30 time between the fast and slow split shear waves (δt) via SKS splitting can help
31 place spatial and temporal constraints on lithospheric deformation. The
32 Canadian Appalachians experienced multiple episodes of deformation during the
33 Phanerozoic: accretionary collisions during the Paleozoic prior to the collision
34 between Laurentia and Gondwana, and rifting related to the Mesozoic opening of
35 the North Atlantic. However, the extent to which extensional events have
36 overprinted older orogenic trends is uncertain. We address this issue through
37 measurements of seismic anisotropy beneath the Canadian Appalachians,
38 computing shear wave splitting parameters (ϕ , δt) for new and existing seismic
39 stations in Nova Scotia and New Brunswick. Average δt values of 1.2 s, relatively
40 short length-scale (≥ 100 km) splitting parameter variations, and a lack of
41 correlation with absolute plate motion direction and mantle flow models,
42 demonstrate that fossil lithospheric anisotropic fabrics dominate our results.
43 Most fast directions parallel Appalachian orogenic trends observed at the
44 surface, while δt values point towards coherent deformation of the crust and
45 mantle lithosphere. Mesozoic rifting had minimal impact on our study area,
46 except locally within the Bay of Fundy and in southern Nova Scotia, where fast
47 directions are sub-parallel to the opening direction of Mesozoic rifting;
48 associated δt values of >1 s require an anisotropic layer that spans both the crust

49 and mantle, meaning the formation of the Bay of Fundy was not merely a thin-
50 skinned tectonic event.

51

52 **Keywords:**

53 102. Seismic anisotropy

54 111. Body waves

55 141. Continental tectonics: compressional

56 142. Continental tectonics: extensional

57 206. North America

58

59

60

61

62

63

64 **Introduction**

65

66 Plate scale deformation can lead to the development of an anisotropic fabric
67 within the lithosphere (e.g. Helffrich, 1995) through the alignment of olivine
68 crystals in the upper mantle (e.g., Bystricky et al., 2000; Tommasi et al., 2000;
69 Zhang and Karato, 1995). When a shear wave travels through an anisotropic
70 medium it is split into two orthogonal shear waves, one travelling faster than the
71 other (e.g., Silver 1996). Measurements of the polarisation direction of the fast
72 wave (ϕ) and the delay time between the fast and slow waves (δt) can then be
73 used to characterise the anisotropic medium.

74

75 Core shear waves such as SKS and SKKS (hereafter referred to as SKS) are well
76 suited for studying shear wave splitting and the anisotropic properties of the
77 upper mantle directly beneath a seismic station. They are radially polarised, P-
78 to-S conversions formed at the core-mantle boundary that preserve no source-
79 side anisotropy (Long and Silver 2009, Savage 1999).

80

81 The Canadian Appalachians have experienced multiple episodes of deformation
82 during the Phanerozoic (e.g. van Staal and Barr, 2012). A series of Paleozoic
83 accretionary collisions took place on the margin of Laurentia, prior to the
84 Laurentia-Gondwana collision that formed the supercontinent Pangea. In the
85 Mesozoic, rifting related to the opening of the North Atlantic affected the eastern
86 edge of this region, one consequence of which was the formation of the Bay of
87 Fundy (e.g. Withjack et al., 1995) (Figure 1).

88

89 Previous studies of shear-wave splitting parameters in southeast Canada
90 revealed little correspondence between orientations of anisotropic fabrics and
91 asthenospheric flow beneath the Canadian Appalachians (Darbyshire et al.,
92 2015). Fossil lithospheric anisotropic fabrics are thus likely to exert first order
93 control on the observations. However, data from only a small number of seismic
94 stations in the Canadian Appalachians have been used to establish this
95 hypothesis, rendering the plate-scale tectonic evolution of the region poorly
96 constrained in space and time. For example, whether or not the Mesozoic
97 formation of the Fundy Basin was a thin-skinned, 'crustal' event, or one that also
98 affected the mantle lithospheric mantle, remains poorly understood.

100 To address these issues, we analyse broadband seismic data from a combined
101 network of new and existing seismic stations centred on the Bay of Fundy, to
102 compute shear wave splitting parameters (ϕ , δt) for the region. After
103 consideration of proposed mantle flow directions from absolute plate motion
104 (APM) and geodynamic modelling results (Darbyshire et al., 2015), we compare
105 the orientation of the fast direction to geological trends from the Appalachian
106 orogenies, rifting in the Bay of Fundy, and extension related to the opening of the
107 North Atlantic. In doing so, we assess the orientation and depth extent of
108 deformation and whether rifting-related anisotropic fabrics have overprinted
109 older orogenic anisotropic fabrics.

110

111

112

113

114 **Tectonic setting**

115

116 The Canadian Appalachians formed from the accretion of a series of oceanic arcs
117 and continental fragments to the southeast margin of Laurentia during the
118 Paleozoic. The region can be divided into five principal tectonostratigraphic
119 zones (Williams, 1979) (Figure 1), although it should be noted that some
120 comprise distinct tectonic elements themselves (e.g., van Staal and Barr, 2012).
121 To the northwest the Humber Margin, was the edge of Laurentia when Dunnage
122 zone material was accreted during the Ordovician, closing the Taconic Seaway.

123 Both zones comprise material that was on the Laurentian side of the Iapetus
124 Ocean.
125

126 The three southeastern zones, Ganderia, Avalonia and Meguma, were continental
127 fragments that separated from Gondwana during the Early Paleozoic. Ganderia
128 collided with the composite edge of Laurentia during the Silurian, closing the
129 Iapetus Ocean, and Avalonia accreted during the Early Devonian Arcadian
130 Orogeny. Finally, Meguma, a terrane only found in present-day southern Nova
131 Scotia, collided with the Avalonian edge of Laurentia in the Carboniferous.
132

133 Terminal collision between Laurentia and Gondwana occurred in the Mid-
134 Carboniferous and Early Permian during the Alleghanian Orogeny, and led to the
135 formation of the supercontinent Pangea. The Canadian Appalachians were
136 relatively unaffected by Alleghanian Orogeny deformation (van Staal and Barr,
137 2012) and are thus a good location to study structures related to the earlier
138 accretionary tectonic phases.
139

140 During the Mid-Triassic to Early Jurassic, NW-SE oriented rifting formed the Bay
141 of Fundy (Withjack et al. 1995, Withjack et al. 2010). Rifting reactivated
142 Paleozoic thrusts as normal faults, and resulted in the deposition of synrift non-
143 marine sedimentary rocks and the eruption of tholeiitic basalts (Withjack et al.
144 1995). Fundy Basin extension ceased with the opening of the North Atlantic in
145 the Early-to-Mid Jurassic. The rifted margin shows variation off-shore of Nova
146 Scotia: the margin is volcanic to the southwest, but non-volcanic to the northeast
147 of Nova Scotia and Newfoundland (Keen and Potter et al., 1995; Funck et al.,

148 2004). Since the Cretaceous, the Canadian Appalachians have been tectonically
149 quiet.

150

151

152

153 **Data and Methods**

154

155 We use data from nineteen broadband seismic stations deployed in the Canadian
156 Appalachians (Table 1, Figure 1) in Nova Scotia, New Brunswick, Newfoundland
157 and Quebec. Of these, nine stations are from the Imperial College Maritimes
158 network in Nova Scotia and New Brunswick, deployed between September 2013
159 and August 2015. These stations consisted of Gralp CMG-3TP seismometers
160 with associated Gralp digitisers and GPS timing. The remaining stations consist
161 of six temporary POLARIS stations (Portable Observatories for Lithospheric
162 Analysis and Research Investigating Seismicity: Eaton et al., 2005) that operated
163 for periods of 2-3.5 years, and four permanent stations from the Canadian
164 National Seismograph Network (CNSN).

165

166 Earthquakes that occurred between October 2005 and October 2015, with
167 magnitudes ≥ 6.0 and epicentral distances $\geq 88^\circ$ were selected from the global
168 catalogue. This distance range was chosen to isolate SKS core phases from other
169 direct S phases to focus our analysis on receiver-side mantle anisotropy.

170 Seismograms were filtered using a zero-phase, two-pole, Butterworth band-pass
171 filter with corner frequencies 0.04 and 0.3 Hz. Seismograms were visually

172 inspected and waveforms with high signal-to-noise ratio, where an SKS or SKKS
173 phase was clearly visible, were selected for further analysis.

174

175

176 When an SKS phase exhibits shear wave splitting, particle motion is elliptical
177 because a proportion of the energy exists on the tangential component (e.g.
178 Figure 2). If shear wave splitting does not occur, the particle motion will be
179 linear and no energy appears on the tangential component, resulting in a 'null'
180 measurement (e.g. Figure 3). A null may result from the material that the wave
181 passes through being azimuthally-isotropic, multiple layers of anisotropy
182 cancelling out (Barruol and Hoffmann, 1999), or if the backazimuth of the
183 incoming earthquake is parallel or perpendicular to the fast polarisation
184 direction.

185

186 We measure the fast polarisation direction (ϕ) and the delay time between the
187 fast and slow shear waves (δt) using the approach of Teanby et al., (2004), which
188 is based on the methodology of Silver and Chan (1991). Horizontal-component
189 seismograms are rotated and time-shifted to minimise the second eigenvalue of
190 the covariance matrix for particle motion within a window around the SKS
191 phase. This is equivalent to linearising particle motion, and minimising the
192 energy on the tangential component seismogram. We make measurements for
193 100 different windows around the SKS phase, and use cluster analysis to
194 determine the most stable splitting parameters. Only measurements where the
195 difference between the back-azimuth and source polarisation direction of the
196 SKS phase is $\leq 20^\circ$ are accepted, thus avoiding spurious results that could be

197 associated with anomalies in the deep lower mantle (e.g., Restivo and Helffrich,
198 2006). We obtain 40 high quality split measurements and 30 null measurements
199 from 25 earthquakes (Tables S1 and S2, Figure 4). It should be noted that many
200 of the seismic stations were located close to the coast, in a relatively high noise
201 environment, and some stations (e.g. ALLY, JOSY, MANY) only operated for the
202 short timespan of ~ 1 year.

203

204

205

206 **Results**

207

208 Figure 2 shows an example of a split measurement from station EDEY; Figure 3 is
209 an example null measurement from station SJNN. Splitting parameters for
210 individual station-event pairs are shown in Figures S1-4 and summarised in
211 Figure S5 and Table S2.

212

213 At stations where splitting parameters show no significant backazimuthal
214 variation, mantle anisotropy is characterised as a single, homogenous, horizontal
215 layer; we thus adopt the stacking approach of Restivo and Helffrich (2006) to
216 obtain a single pair of splitting parameters. Data coverage is insufficient to
217 resolve the complex patterns of shear wave splitting variation associated with
218 multiple or dipping anisotropic layers.

219

220 Results are summarised in Figure 4 and Table 1. Delay times range from 0.7 s
221 (TIGG) to 1.85 s (MALG), but most fall within $\delta t=0.9-1.4$ s. Consistent fast

222 directions can be observed within some groups of stations on a 200-300 km
223 length-scale, but changes over short distances (<100 km) are also evident. One of
224 the most striking is the change from a SE-NW fast direction for stations ALLY
225 (southern Nova Scotia) and MANY (Bay of Fundy) to a SW-NE fast direction for
226 stations in southern New Brunswick (Figure 4). Fast directions across northern
227 Nova Scotia are generally ~WSW-ENE, but those observed for stations CHEG
228 (Cape Breton Island) and TIGG (Prince Edward Island) are NW-SE. The fast
229 direction changes once again to SW-NE on the southern tip of Newfoundland
230 (Figure 4).

231

232 At stations SABG, JOSY, MADG, SJNN and DRLN only null measurements were
233 found. For JOSY, MADG and DRLN, the earthquake backazimuths yielding these
234 results were either parallel or perpendicular to the fast directions observed at
235 neighbouring stations (ALLY and MANY, TIGG and CHEG, and CODG
236 respectively). Given the 90° ambiguity inherent in null measurements, it is
237 reasonable to assume that the null directions are either perpendicular or parallel
238 to the fast direction of anisotropy at these stations. However, the limited
239 backazimuthal coverage means we cannot preclude the presence of multiple,
240 cancelling layers of anisotropy (e.g., Barruol & Hoffmann, 1999) beneath these
241 stations.

242

243

244

245

246

247 **Discussion**

248

249 *Causes of seismic anisotropy and comparisons with previous studies*

250

251 Seismic anisotropy in the Earth results from the alignment of minerals in the
252 crust and/or mantle, the preferential alignment of fluid or melt (e.g., Blackman
253 and Kendall, 1997), alternating sequences of sub-parallel layers of rocks of
254 different seismic velocities (periodic transverse layering; Backus, 1962), or
255 some combination thereof. We exclude melt alignment as a source of anisotropy
256 in the Canadian Appalachians, since the region last experienced magmatism
257 during the Mesozoic (van Staal and Barr, 2012). Mantle anisotropy therefore
258 most likely results from the alignment of olivine crystals, olivine being the most
259 abundant mineral in the upper mantle and highly anisotropic. Shear stresses can
260 lead to the development of crystallographic preferred orientation (CPO) of
261 olivine, where the a-axis is aligned to an orientation related to deformation (e.g.,
262 Bystricky et al., 2000; Tommasi et al., 2000; Zhang and Karato, 1995).

263

264 Processes that could lead to the development of anisotropic fabric include:
265 asthenospheric flow in the direction of APM (e.g., Bokermann and Silver, 2002),
266 asthenospheric flow around a cratonic root (e.g., Assumpção et al., 2006;
267 Bormann et al., 1993), and frozen-in fossil anisotropy within the lithosphere
268 from the last deformation event (e.g., Bastow et al., 2007; Silver and Chan, 1988;
269 Vauchez and Nicolas, 1991).

270

271 Periodic transverse layering is likely a source of anisotropy at crustal depths,
272 however the continental crust typically only accounts for only 0.1-0.3 s (Silver,
273 1996) or 0.1-0.5 s (Barruol and Mainprice, 1993) of SKS splitting observations,
274 so our δt values (mean $\delta t=1.2$ s) require a mantle contribution. Estimates of
275 anisotropic layer thickness can be made from the relationship $L \approx (\delta t * V_s)/dV_s$
276 (e.g., Helffrich, 1995), where L is layer thickness, V_s is shear velocity, and dV_s is
277 average percentage anisotropy. Taking a dV_s of 4%, an upper limit of the degree
278 of anisotropy prevalent in the upper 200 km of the Earth, (Savage, 1999) and a
279 V_s in the range 4.48 km/s (mantle velocities from ak135, Kennett et al. 1995) to
280 4.65 km/s (average cratonic lithospheric mantle velocities in SE Canada
281 (Schaeffer and Lebedev, 2014, Yuan et al., 2014)), our mean $\delta t=1.2$ s corresponds
282 to a layer thickness of 134-140 km, not dissimilar to the ~ 150 -175 km estimates
283 for lithospheric thickness in the Canadian Appalachians (Schaeffer and Lebedev,
284 2014). Similarly, if we assume that the average 1.2 s of splitting we observe is
285 accrued in the region's 150-175 km thick lithosphere (e.g., Schaeffer and
286 Lebedev, 2014), the uppermost mantle beneath our network would be, on
287 average, 3.1-3.7% anisotropic, a reasonable estimate for lithospheric anisotropy
288 when compared to other studies worldwide (e.g. Savage, 1999). Further, the
289 distances over which splitting parameters change (in several cases <100 km) is
290 smaller than the width of the first Fresnel zone at the base of the lithosphere
291 (~ 150 km).

292

293 There are four published SKS splitting measurements in our study area from
294 Darbyshire et al. (2015) (Figure 4, Table 1). These show good agreement with
295 the results we obtain from nearby stations. The nearest station to our region

296 analysed by Barruol et al. (1997) (station CBM in Maine) has a similar fast
297 direction to that of station HOLY, and is sub-parallel to the strike of Paleozoic
298 Appalachian orogenic structures.

299

300 Many of the ϕ measurements obtained from the northern US Appalachians to
301 the southwest of our study region by Barruol et al. (1997) are E-W oriented.
302 Subsequent modelling of anisotropy in the New England region (Levin et al.,
303 1999; Levin et al., 2000; Yuan and Levin, 2014) finds that it is best explained by
304 two distinct layers: a lower layer in the asthenosphere paralleling APM, and an
305 upper layer in the lithosphere that is perpendicular to the main geological trends
306 in the region. It is argued that this upper layer may be a result of a fabric
307 developed due to the loss of the lower part of the lithosphere at some point after
308 the assemblage of the Appalachians. Multiple layers of anisotropy, including the
309 presence of anisotropy in the lithosphere, are further supported by estimates of
310 anisotropic parameters made using splitting measurements and full waveform
311 analysis (e.g., Yuan and Romanowicz, 2010; Yuan et al., 2011).

312

313 Long et al. (2015) recently conducted an SKS splitting study of the eastern US
314 using data from the Transportable Array seismic stations. In the southern
315 Appalachians, from Alabama to Pennsylvania, they see a strong correlation
316 between ϕ and the strike of the mountain chain, including a rotation in ϕ
317 coincident with a bend in topography. They argue in this region that the primary
318 contribution to anisotropy is from the lithosphere. In the region closest to our
319 study region, directly to the west and south, their results are more complex.
320 Averaged over a relatively large area, the average ϕ direction is 77° , however

321 there is significant variation over relatively short distances, which they also
322 argue suggests a lithospheric component to the observed anisotropy. In neither
323 of these two regions do they observe a consistent alignment to APM.

324

325 *Role of plate motion and mantle flow*

326

327 Splitting measurements from southern New Brunswick and southern
328 Newfoundland show some agreement with the APM direction from the HS3-
329 NUVEL 1A (hotspot) model (Gripp and Gordon, 2002), however there is no
330 consistent correlation with APM direction across the whole region. Similarly,
331 while the fast direction observed in southern Nova Scotia and in the Bay of
332 Fundy parallels the NNR-MORVEL (no-net-rotation) model (DeMets et al., 2010)
333 there is again no consistent correlation throughout the Maritimes. Furthermore,
334 the North American Plate is moving relatively slowly (17-22 mm/yr), slower
335 than the ~40 mm/yr that Debayle and Ricard (2013) suggest is the necessary
336 plate velocity for basal drag fabrics to develop based on their global comparison
337 of APM and anisotropic fast directions. Anisotropy resulting from APM is,
338 therefore, unlikely to be the dominant cause of the observed anisotropy.

339

340 Darbyshire et al. (2015) compare splitting parameters to mantle flow predictions
341 of Forte et al. (2015). In the model that best simulates the lithospheric thickness
342 in Appalachian Canada, radial flow dominates over horizontal flow. This would
343 result in null measurements for the majority of seismic stations in this region:
344 this clearly is not the case for most stations. Taking into account our estimates of
345 anisotropic layer thickness and the lack of correlation of APM directions and

346 mantle flow models, a fossil lithospheric hypothesis for Canadian Appalachian
347 mantle anisotropy seems most appropriate.

348

349 Backazimuthal coverage of our splitting measurements is limited to a relatively
350 narrow range (Figures S1-S4). Studies with better backazimuthal representation
351 are usually associated with stations that operated for much longer than the 1-3
352 years to which we have access (e.g., Levin et al., 2000). Although our
353 interpretations are necessarily limited to a single homogenous, horizontal layer
354 of anisotropy, we cannot preclude the possibility of dipping or multiple layers of
355 anisotropy, including an asthenospheric component (e.g. Levin et al., 2000; Silver
356 and Savage, 1994).

357

358

359 *Relationship with tectonic structures*

360

361 Fast polarisation directions in the Canadian Appalachians are mostly parallel or
362 subparallel to geological trends from the Paleozoic Appalachian orogenies
363 (Figure 1). Variations, such as between those in southern New Brunswick and
364 those in Nova Scotia, and between Prince Edward Island, New Brunswick and
365 Newfoundland follow variations in the strike of the boundaries between the
366 different tectonic zones. Agreement between Appalachian trends and fast
367 directions has also been documented elsewhere in the orogen by Long et al.
368 (2015) and in earlier work by Barruol et al. (1997). Further, previous SKS
369 splitting studies from other old orogenic belts, such as the Caledonian trends in
370 the UK and Ireland (e.g. Helffrich 1995; Bastow et al., 2007) have also noted that

371 olivine CPO tends to parallel the strike of these belts. Much of the anisotropy we
372 observe is thus related to Appalachian tectonic deformation. Splitting delay
373 times of $\delta t > 1$ s point towards plate-scale deformation, coherent in the crust and
374 lithospheric mantle.

375

376 The NW-SE fast direction at station MANY in the Bay of Fundy is at a high angle
377 to the trend of Appalachian structures. The Bay of Fundy underwent rifting in a
378 NW-SE direction during the Mid-Triassic to Early Jurassic (e.g. Withjack et al.
379 1995); extensional deformation may thus have over-printed older Appalachian
380 trends. In magma-rich rifts, fast directions are typically rift-parallel (e.g., Kendall
381 et al., 2006), but in magma-poor rifts such as the Rhine Graben (Vinnik et al.,
382 1992) and the Baikal rift (Gao et al., 1997), they tend to be rift-perpendicular.
383 This is due to the lattice-preferred orientation of lithospheric mantle olivine
384 crystals induced by plate stretching (Nicolas and Christensen, 1987). Withjack et
385 al. (1995) suggest the Fundy Basin experienced compression in a NW-SE
386 direction from the Early Jurassic to Early Cretaceous. Unlike the earlier rifting,
387 this does not seem to have influenced the lithospheric mantle.

388

389 The fast direction for MANY is slightly oblique ($\sim 25^\circ$) to the Bay of Fundy paleo
390 opening direction. Obliquity between the strike of normal fault networks and
391 opening directions is not uncommon during the development of continental
392 breakup, however. For example, Corti et al., (2008) observe a $\sim 20^\circ$ obliquity in
393 the tectonically active Ethiopian rift. Our observations are thus consistent with
394 the hypothesis that, in the Bay of Fundy, Mesozoic plate-scale extensional
395 tectonics over-printed older Appalachian fossil lithospheric anisotropic fabrics.

396

397 The fast direction at ALLY on the Atlantic coast of southern Nova Scotia is similar
398 to MANY, but $\sim 30^\circ$ different to HAL, also located on Nova Scotia's Atlantic coast.

399 The observations at ALLY may, like MANY, be the result of Mesozoic rifting.

400 Although we cannot constrain them, along-axis variations in the strength of the
401 continental lithosphere may explain our observations: weaker lithosphere to the
402 south where the Bay of Fundy formed; stronger lithosphere to the north.

403 Offshore rifted margin structure lends some support to this hypothesis: seaward
404 dipping reflector sequences are prevalent along the margin in the south, but
405 missing further northeast (Keen and Potter et al., 1995). Funck et al. (2004)
406 argue that the Nova Scotian margin becomes increasingly non-volcanic to the
407 northeast, also implying a change in extensional processes along-strike.

408 Regardless of the governing factor, we conclude that Mesozoic extensional
409 deformation of the lithosphere in the Canadian Maritimes was plate-scale but
410 localised in nature.

411

412

413

414

415

416 **Conclusions**

417

418 SKS splitting measurements are made at nineteen broadband seismic stations in
419 the Canadian Appalachians. Improved station numbers and density compared to
420 previous studies in this region means we are better able to constrain spatial and

421 temporal variations in lithospheric deformation. The length scale of variations
422 (~100 km), average δt of 1.2 s, and the lack of correlation with APM directions
423 and asthenospheric flow models suggests that frozen-in lithospheric fabrics
424 dominate the anisotropy in the region. There is good agreement between the fast
425 polarisation directions at most stations and surface geological trends related to
426 the Appalachian orogenies. Paleozoic accretionary collisions thus likely
427 deformed the crust and the mantle lithosphere coherently. Later Mesozoic rifting
428 had minimal impact on the Canadian Appalachians outside of the Bay of Fundy
429 and southern Nova Scotia. In these areas, fast directions do not follow
430 Appalachian trends, but are sub-parallel to the direction of rifting in the
431 Mesozoic. This suggests that Mesozoic rifting affected the entire lithosphere
432 beneath the Bay of Fundy, not just the crust, but its influence was confined to this
433 relatively small area.

434

435

436

437 **Acknowledgements**

438

439 This work was funded by Leverhulme Trust research project grant RPG-2013-
440 332. Imperial College Maritimes network stations were provided through [NERC](#)
441 Geophysical Equipment Facility loan 986. Logistical field support was provided
442 by D. Heffler, D. Simpson and residents of Nova Scotia and New Brunswick. Data
443 for POLARIS and CNSN stations were downloaded from the Canadian National
444 Data Centre. POLARIS stations were funded by the Canadian Foundation for
445 Innovation, Natural Resources Canada and Industry Canada. F.D. is supported by

446 NSERC through the Discovery Grants and Canada Research Chair programmes.
447 A.B. is funded by the NERC Doctoral Training Partnership: Science and Solutions
448 for a Changing Planet. We thank Thomas Plenefisch and an anonymous reviewer
449 for their comments on this manuscript.

450

451

452

453

454

455

456

457

458

459

460

461

462 **References**

463

464

465 Assumpção, M., Heintz, M., Vauchez, A., & Silva, M. E. (2006). Upper mantle
466 anisotropy in SE and Central Brazil from SKS splitting: evidence of
467 asthenospheric flow around a cratonic keel. *Earth and Planetary Science Letters*,
468 250(1), 224-240. doi:10.1016/j.epsl.2006.07.038

469

470 Backus, G. E. (1962), Long-wave elastic anisotropy produced by horizontal

471 layering, *Journal of Geophysical Research*, 67, 4427– 4440.

472

473 Barruol, G., & Mainprice, D. (1993). A quantitative evaluation of the contribution
474 of crustal rocks to the shear-wave splitting of teleseismic SKS waves. *Physics of*
475 *the Earth and Planetary Interiors*, 78(3), 281-300. doi:10.1016/0031-

476 9201(93)90161-2

477

478

479 Barruol, G., Silver, P. G., & Vauchez, A. (1997). Seismic anisotropy in the eastern
480 United States: deep structure of a complex continental plate. *Journal of*

481 *Geophysical Research*, 102, 8329-8348. doi: 10.1029/96JB03800

482

483 Barruol, G., & Hoffmann, R. (1999). Upper mantle anisotropy beneath the
484 Geoscope stations. *Journal of Geophysical Research*, 104(B5), 10757-10. doi:

485 10.1029/1999JB900033

486 Bastow, I. D., Owens, T. J., Helffrich, G., & Knapp, J. H. (2007). Spatial and
487 temporal constraints on sources of seismic anisotropy: Evidence from the
488 Scottish highlands. *Geophysical Research Letters*, 34, L05305,

489 doi:10.1029/2006GL028911

490 Blackman, D. K., & Kendall, J. M. (1997). Sensitivity of teleseismic body waves to
491 mineral texture and melt in the mantle beneath a mid-ocean ridge. *Philosophical*

492 *Transactions of the Royal Society of London A: Mathematical, Physical and*

493 *Engineering Sciences*, 355(1723), 217-231. doi: 10.1098/rsta.1997.0007

494

495 Bokermann, G., and Silver, P., 2002, Shear stress at the base of shield lithosphere:
496 *Geophysical Research Letters*, 29(23), 2091, doi: 10.1029/2002GL015925.
497

498 Bormann, P., Burghardt, P. T., Makeyeva, L. I., & Vinnik, L. P. (1993). Teleseismic
499 shear-wave splitting and deformations in Central Europe. *Physics of the Earth*
500 *and Planetary Interiors*, 78(3), 157-166. doi:10.1016/0031-9201(93)90153-Z
501

502 Bystricky, M., Kunze, K., Burlini, L., & Burg, J. P. (2000). High shear strain of
503 olivine aggregates: rheological and seismic consequences. *Science*, 290(5496),
504 1564-1567. doi: 10.1126/science.290.5496.1564
505

506 Corti, G. (2008). Control of rift obliquity on the evolution and segmentation of the
507 main Ethiopian rift. *Nature Geoscience*, 1(4), 258-262. doi:10.1038/ngeo160
508

509 Darbyshire, F. A., Bastow, I. D., Forte, A. M., Hobbs, T. E., Calvel, A., Gonzalez-
510 Monteza, A., & Schow, B. (2015). Variability and origin of seismic anisotropy
511 across eastern Canada: evidence from shear-wave splitting measurements.
512 *Journal of Geophysical Research*, 120, doi:10.1002/2015JB012228
513

514 Debayle, E., & Ricard, Y. (2013). Seismic observations of large-scale deformation
515 at the bottom of fast-moving plates. *Earth and Planetary Science Letters*, 376,
516 165-177. doi:10.1016/j.epsl.2013.06.025
517

518 DeMets, C., Gordon, R. G., & Argus, D. F. (2010). Geologically current plate
519 motions. *Geophysical Journal International*, 181(1), 1-80. doi: 10.1111/j.1365-
520 246X.2009.04491.x

521

522 Eaton, D. W., Adams, J., Asudeh, I., Atkinson, G. M., Bostock, M. G., Cassidy, J. F.,
523 Ferguson, I., Samson, C., Snyder, D., Tiampo, K.F., & Unsworth, M. J. (2005).
524 Investigating Canada's lithosphere and earthquake hazards with portable arrays.
525 *Eos, Transactions American Geophysical Union*, 86(17), 169-173. doi:
526 10.1029/2005E0170001

527

528 Forte, A. M., Simmons, N. A., & Grand, S. P. (2015). Constraints on seismic models
529 from other disciplines—Constraints on 3-D seismic models from global
530 geodynamic observables: Implications for the global mantle convective flow.
531 *Treatise of Geophysics*, 1, 853-907.

532

533 Funck, T., Jackson, H. R., Louden, K. E., Dehler, S. A., & Wu, Y. (2004). Crustal
534 structure of the northern Nova Scotia rifted continental margin (eastern
535 Canada). *Journal of Geophysical Research*, 109, B09102,
536 doi:10.1029/2004JB003008

537

538 Gao, S., Davis, P.M., Liu, H., Slack, P.D., Rigor, A.W., Zorin, Y.A., Mordvinova, V.V.,
539 Kozhevnikov, V.M. & Logatchev, N.A. (1997). SKS splitting beneath continental
540 rift zones. *Journal of Geophysical Research*, 102(B10), 22781-22797. doi:
541 10.1029/97JB01858

542

543 Gripp, A. E., & Gordon, R. G. (2002). Young tracks of hotspots and current plate
544 velocities. *Geophysical Journal International*, 150(2), 321-361. doi:
545 10.1046/j.1365-246X.2002.01627.x
546
547 Helffrich, G. (1995). Lithospheric deformation inferred from teleseismic shear
548 wave splitting observations in the United Kingdom. *Journal of Geophysical*
549 *Research*, 100(B9), 18195-18204. doi: 10.1029/95JB01572
550
551 Keen, C. E., & Potter, D. P. (1995). The transition from a volcanic to a nonvolcanic
552 rifted margin off eastern Canada. *Tectonics*, 14(2), 359-371. doi:
553 10.1029/94TC03090
554
555 Kendall, J. M., Pilidou, S., Keir, D., Bastow, I. D., Stuart, G. W., & Ayele, A. (2006).
556 Mantle upwellings, melt migration and the rifting of Africa: insights from seismic
557 anisotropy. *Geological Society, London, Special Publications*, 259(1), 55-72. doi:
558 10.1144/GSL.SP.2006.259.01.06
559
560 Kennett, B. L. N., Engdahl, E. R., and Buland, R., (1995), Constraints on seismic
561 velocities in the Earth from traveltimes. *Geophysical Journal International*, 122
562 (1): 108-124. doi: 10.1111/j.1365-246X.1995.tb03540.x
563
564 Levin, V., Menke, W., & Park, J. (1999). Shear wave splitting in the Appalachians
565 and the Urals: a case for multilayered anisotropy. *Journal of Geophysical*
566 *Research*, 104(B8), 17975-17993. doi: 10.1029/1999JB900168
567

568 Levin, V., Park, J., Brandon, M. T., & Menke, W. (2000). Thinning of the upper
569 mantle during late Paleozoic Appalachian orogenesis. *Geology*, 28(3), 239-242.
570 doi: 10.1130/0091-7613(2000) 28<239:TOTUMD> 2.0.CO;2
571

572 Long, M. D., Jackson, K. G., & McNamara, J. F. (2015). SKS splitting beneath
573 Transportable Array stations in eastern North America and the signature of past
574 lithospheric deformation. *Geochemistry, Geophysics, Geosystems*, 16,
575 doi:10.1002/2015GC006088.
576

577 Long, M. D., & Silver, P. G. (2009). Shear wave splitting and mantle anisotropy:
578 measurements, interpretations, and new directions. *Surveys in Geophysics*, 30(4-
579 5), 407-461. doi: 10.1007/s10712-009-9075-1
580

581 Nicolas, A. and Christensen, N. I. (1987) Formation of Anisotropy in Upper
582 Mantle Peridotites - A Review, in *Composition, Structure and Dynamics of the*
583 *Lithosphere-Asthenosphere System (eds K. Fuchs and C. Froidevaux)*, 111-123,
584 doi: 10.1029/GD016p0111
585

586 Restivo, A., & Helffrich, G. (2006). Core—mantle boundary structure investigated
587 using SKS and SKKS polarization anomalies. *Geophysical Journal International*,
588 165(1), 288-302. doi: 10.1111/j.1365-246X.2006.02901.x
589

590 Schaeffer, A. J., & Lebedev, S. (2014). Imaging the North American continent
591 using waveform inversion of global and USArray data. *Earth and Planetary*
592 *Science Letters*, 402, 26-41. doi:10.1016/j.epsl.2014.05.014

593

594 Savage, M. K. (1999). Seismic anisotropy and mantle deformation: what have we
595 learned from shear waves. *Reviews of Geophysics*, 37(1), 65-106. doi:

596 10.1029/98RG02075

597

598 Silver, P. G., & Chan, W. W. (1988). Implications for continental structure and
599 evolution from seismic anisotropy. *Nature*, 335, 34-39 doi:10.1038/335034a0

600

601 Silver, P. G., & Chan, W. W. (1991). Shear wave splitting and subcontinental
602 mantle deformation. *Journal of Geophysical Research*, 96(16), 16429-16454. doi:

603 10.1029/91JB00899

604

605 Silver, P. G., & Savage, M. K. (1994). The interpretation of shear-wave splitting
606 parameters in the presence of two anisotropic layers. *Geophysical Journal*

607 *International*, 119(3), 949-963. doi: 10.1111/j.1365-246X.1994.tb04027.x

608

609 Silver, P. G. (1996). Seismic anisotropy beneath the continents: probing the
610 depths of geology. *Annual Review of Earth and Planetary Sciences*, 24, 385-432.

611 doi: 10.1146/annurev.earth.24.1.385

612

613 Teanby, N. A., Kendall, J. M., & Van der Baan, M. (2004). Automation of shear-
614 wave splitting measurements using cluster analysis. *Bulletin of the Seismological*

615 *Society of America*, 94(2), 453-463. doi: 10.1785/0120030123

616

617 Tommasi, A., Mainprice, D., Canova, G., & Chastel, Y. (2000). Viscoplastic self-
618 consistent and equilibrium-based modeling of olivine lattice preferred
619 orientations: Implications for the upper mantle seismic anisotropy. *Journal of*
620 *Geophysical Research*, 105(B4), 7893-7908. doi: 10.1029/1999JB900411
621

622 van Staal, C. R., & Barr, S. M. (2012). Lithospheric architecture and tectonic
623 evolution of the Canadian Appalachians and associated Atlantic margin. *Tectonic*
624 *styles in Canada: The LITHOPROBE perspective*. Edited by JA Percival, FA Cook, and
625 RM Clowes. *Geological Association of Canada, Special Paper, 49*, 41-95.
626

627 Vauchez, A., & Nicolas, A. (1991). Mountain building: strike-parallel motion and
628 mantle anisotropy. *Tectonophysics*, 185(3), 183-201. doi:10.1016/0040-
629 1951(91)90443-V
630

631

632 Vinnik, L. P., Makeyeva, L. I., Milev, A., & Usenko, A. Y. (1992). Global patterns of
633 azimuthal anisotropy and deformations in the continental mantle. *Geophysical*
634 *Journal International*, 111(3), 433-447. doi: 10.1111/j.1365-
635 246X.1992.tb02102.x
636

637 Williams, H. (1979). Appalachian orogen in Canada. *Canadian Journal of Earth*
638 *Sciences*, 16(3), 792-807. doi: 10.1139/e79-070
639

640 Withjack, M. O., Olsen, P. E. and Schlische, R. W. (1995). Tectonic evolution of the
641 Fundy rift basin, Canada: evidence of extension and shortening during passive
642 margin development. *Tectonics*, 14(2), 390-405. doi: 10.1029/94TC03087
643
644 Withjack, M. O., Baum, M. S., & Schlische, R. W. (2010). Influence of preexisting
645 fault fabric on inversion-related deformation: A case study of the inverted Fundy
646 rift basin, southeastern Canada. *Tectonics*, 29, TC6004,
647 doi:10.1029/2010TC002744
648
649 Yuan, H., & Romanowicz, B. (2010). Lithospheric layering in the North American
650 craton. *Nature*, 466(7310), 1063-1068. doi:10.1038/nature09332
651
652 Yuan, H., Romanowicz, B., Fischer, K. M., & Abt, D. (2011). 3-D shear wave
653 radially and azimuthally anisotropic velocity model of the North American upper
654 mantle. *Geophysical Journal International*, 184(3), 1237-1260. doi:
655 10.1111/j.1365-246X.2010.04901.x
656
657 Yuan, H., & Levin, V. (2014). Stratified seismic anisotropy and the lithosphere-
658 asthenosphere boundary beneath eastern North America. *Journal of Geophysical*
659 *Research*, 119(4), 3096-3114. doi: 10.1002/2013JB010785
660
661 Yuan, H., French, S., Cupillard, P. & Romanowicz, B., 2014. Lithospheric
662 expression of geological units in central and eastern North America from full
663 waveform tomography. *Earth and Planetary Science Letters*, 402, 176-186.
664 doi:10.1016/j.epsl.2013.11.057

665

666 Zhang, S., & Karato, S. I. (1995). Lattice preferred orientation of olivine

667 aggregates deformed in simple shear. *Nature*, 375(6534), 774-777.

668 doi:10.1038/375774a0

669

670

671

672 **Tables**

673

674 *Table 1: Stacked split results*

675

Station	Net	Lat (°)	Lon (°)	ϕ (°)	σ_{ϕ} (°)	δt (s)	$\sigma_{\delta t}$	#	Data period
ALLY	IC	43.74	-65.10	-84	1.25	1.43	0.05	2	09/2013-07/2014; 05/2015-08/2015
CHEG	CNSN	46.81	-60.67	-56	12.75	1.00	0.23	1	10/2005-10/2015
CODG	POLARIS	47.84	-59.25	58	4.75	1.02	0.24	1	10/2005-10/2008
EDEY	IC	45.44	-62.32	83	1.75	1.23	0.03	5	09/2013-08/2015
HAL	CNSN	44.64	-63.59	67	2.5	0.90	0.02	4	08/2008-10/2015
HANN	POLARIS	45.88	-66.77	71	2.5	0.93	0.03	2	01/2013-10/2015
HOLY	IC	46.53	-66.46	33	2.5	1.40	0.08	3	09/2013-08/2015
MALG	POLARIS	45.79	-63.33	71	1	1.85	0.13	2	10/2005-10/2008
MALY	IC	45.79	-63.36	83	5.25	1.05	0.06	3	09/2013-08/2015
MANY	IC	44.69	-66.76	-75	1.5	1.48	0.03	3	09/2013-11/2013; 05/2014-08/2015
SHEY	IC	45.13	-61.99	-89	1.75	1.00	0.03	3	09/2013-08/2015
SUSY	IC	45.72	-65.43	58	5.00	1.23	0.06	2	09/2013-08/2015
TIGG	POLARIS	47.00	-64.00	-55	6.75	0.68	0.09	4	09/2005-11/2007
WODY	IC	45.10	-64.66	85	0.75	1.33	0.02	6	09/2013-

									08/2015
<i>Splitting parameters from Darbyshire et al. (2015)</i>									
BATG	POLARIS	47.23	-66.06	-86	5.00	0.53	0.03	6	
GBN	CNSN	45.41	-61.51	-84	1.50	0.68	0.03	7	
GGN	CNSN	45.12	-66.84	67	1.00	1.03	0.03	9	
LMN	CNSN	45.85	-64.81	76	1.75	1.15	0.06	5	

676

677

678 IC: *Imperial College Maritimes network*

679 POLARIS: *Portable Observatories for Lithospheric Analysis and Research*

680 *Investigating Seismicity*

681 CNSN: *Canadian National Seismograph Network*

682 #: *Number of splitting measurements used in a stack*

683 σ : *one standard deviation*

684 The splitting parameters obtained for individual events can be found in Table S1;

685 null events are recorded in Table S2

686

687

688

689 **Figures**

690

691 *Figure 1*

692

693 Locations of broadband seismic stations (magenta triangles), boundaries

694 separating the Humber, Dunnage, Gander, Avalon and Meguma regions (thin

695 black lines) and the Appalachian Front (thick black line). Inset map shows the

696 location of the study region, marked as a red box, within eastern North America.

697 QC – Quebec, NB – New Brunswick, NS- Nova Scotia, PEI – Prince Edward Island,

698 CBI – Cape Breton Island, NF – Newfoundland, BoF – Bay of Fundy.

699

700 *Figure 2*

701

702 An example of a good splitting measurement at station EDEY. (a) The original
703 three component seismogram showing the SKS phase and the window used. (b)
704 The radial and tangential components before (top two) and after correction
705 (bottom two). There is no energy on the corrected tangential component. (c) Top
706 three images show the match between the fast (dashed line) and slow (solid line)
707 waveforms: left is prior to correction (amplitudes normalised) and centre and
708 right are after correction, normalised and true amplitudes respectively. The
709 bottom two images show the elliptical particle motion prior to correction (left)
710 and the linearised particle motion after correction (right). (d) Error and
711 uncertainty calculation (contour labels indicate multiples of one sigma). Here a
712 stable result and a well constrained 95% confidence contour (thick line) indicate
713 a robust measurement. (e) Measurements of ϕ and δt obtained from 100
714 different analysis windows plotted against window number. (f) Cluster analysis
715 of splitting parameters obtained from the 100 windows. Good results are stable
716 over a large number of windows. In (d), (e) and (f) the star marks the values of ϕ
717 and δt taken for this station/event pair.

718

719 *Figure 3*

720

721 An example of a null result at the station SJNN. (a)-(f) as in Figure 2. Note in (b)
722 the lack of energy on the tangential component before and after correction and
723 in (c) the linear particle motion before and after analysis.

724

725 *Figure 4*

726

727 Stacked shear wave splitting parameters from the stations in this study (purple

728 bars) and from Darbyshire et al. (2015) (cyan bars). Red bars are null

729 measurements. APM: absolute plate motion from the HS3-Nuvel-1A model of

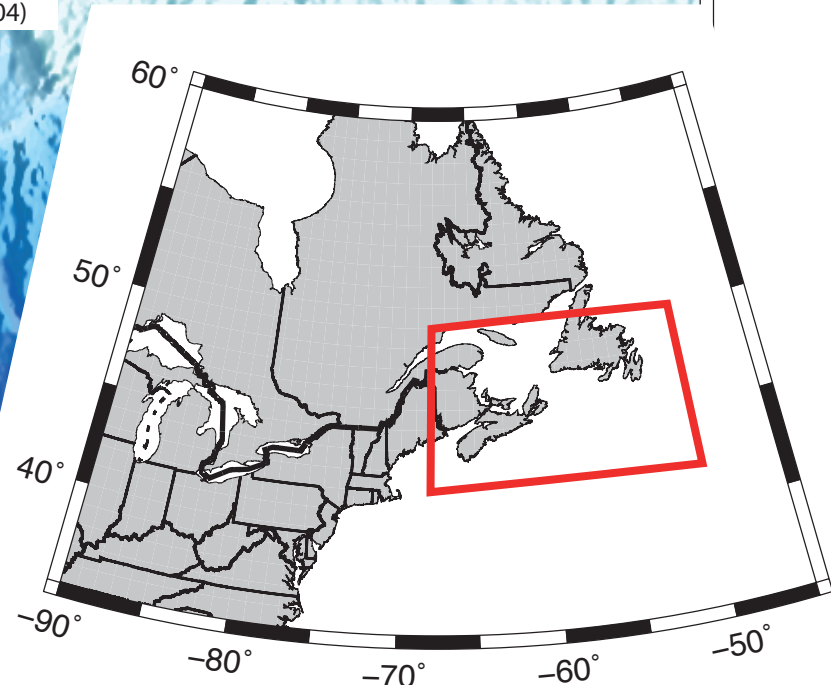
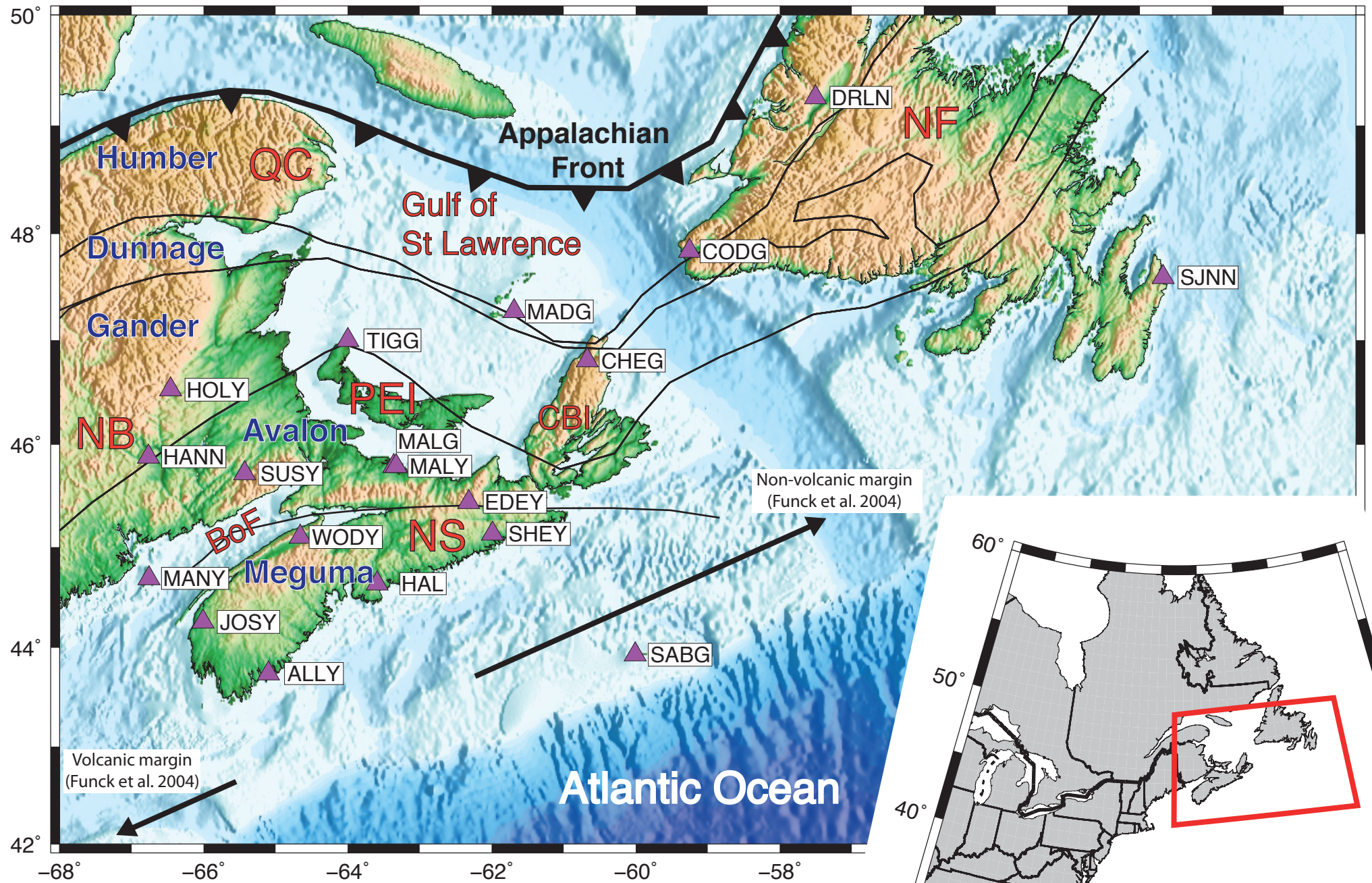
730 Gripp and Gordon (2002) in the hotspot reference frame (black arrow) and the

731 NNR-MORVEL (no-net-rotation) model of DeMets et al. (2010) (green arrow).

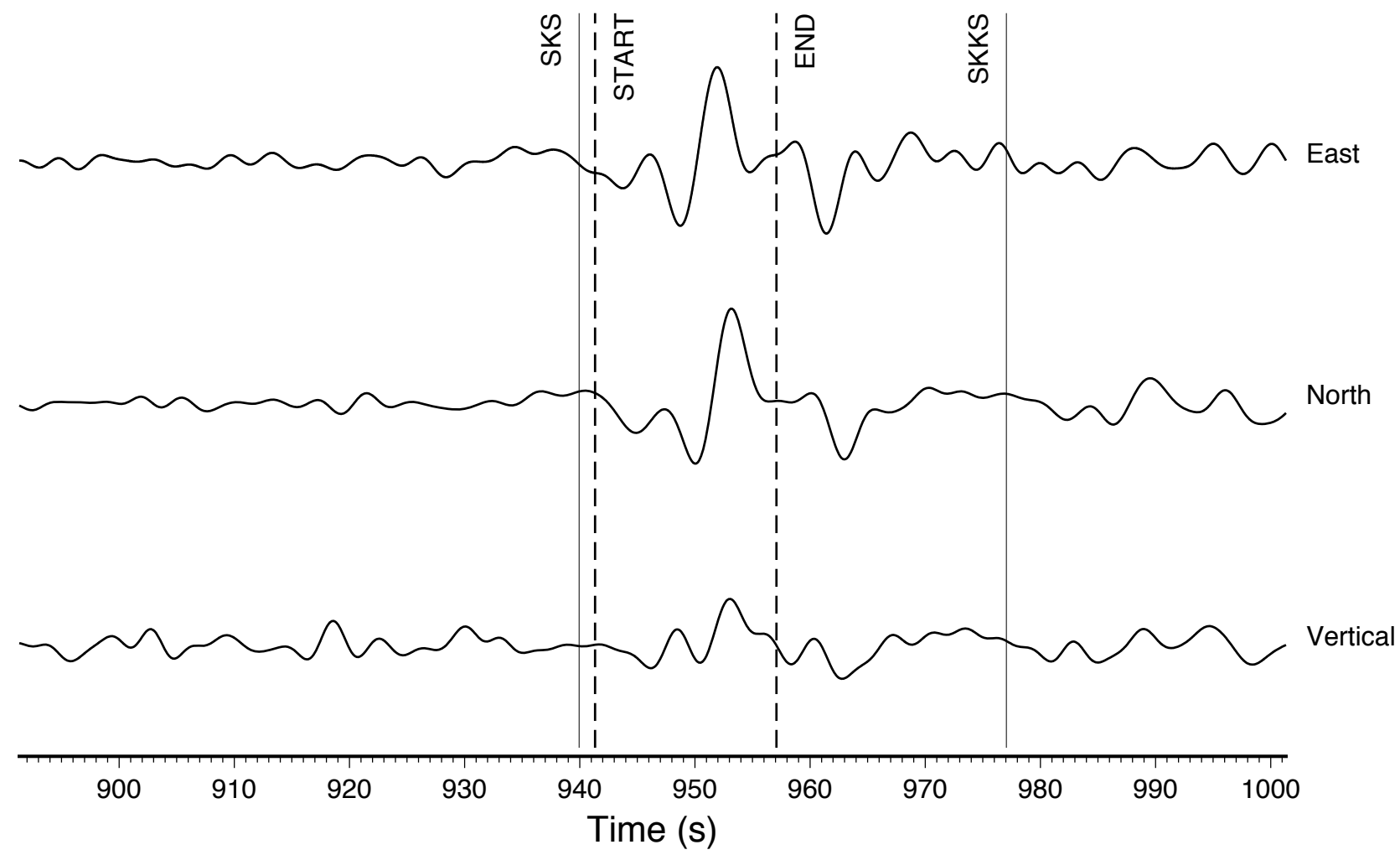
732 Inset map shows the location of earthquakes used; red stars are events where

733 null measurements were obtained and purple stars are events where split

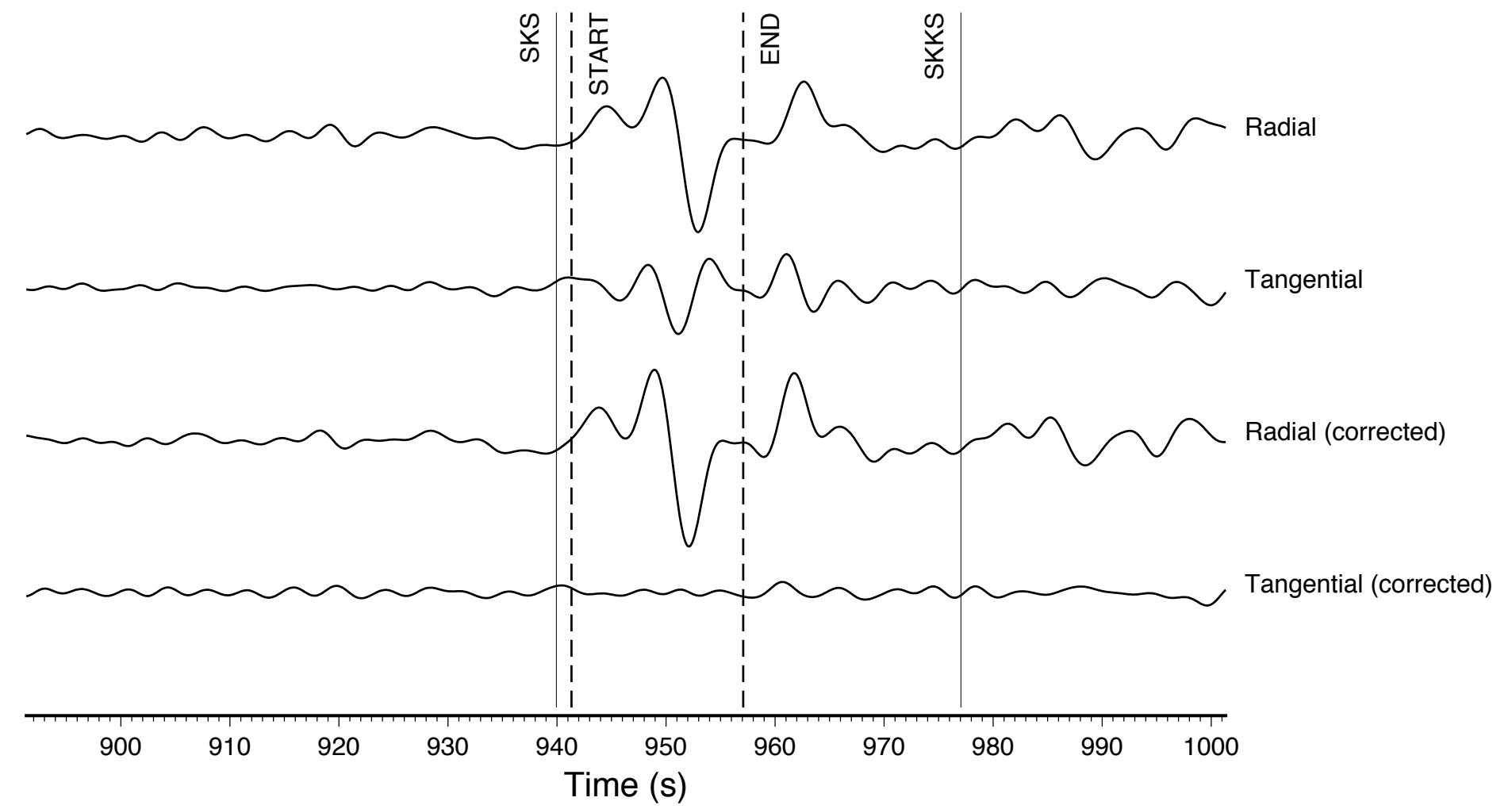
734 measurements were obtained.



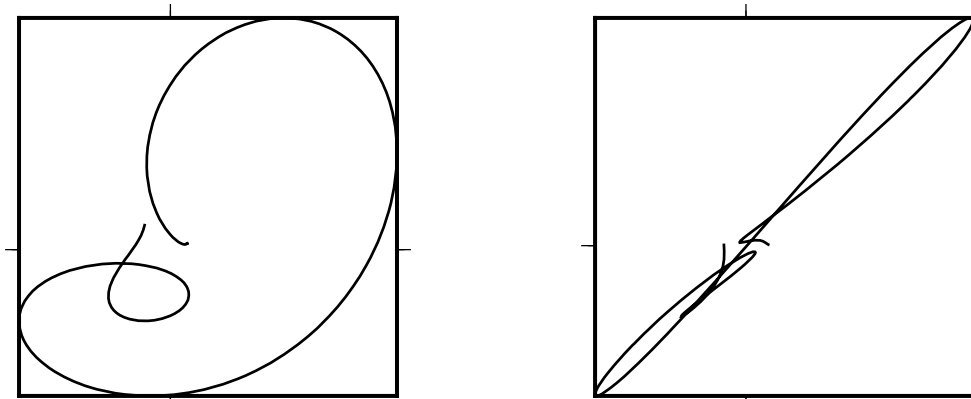
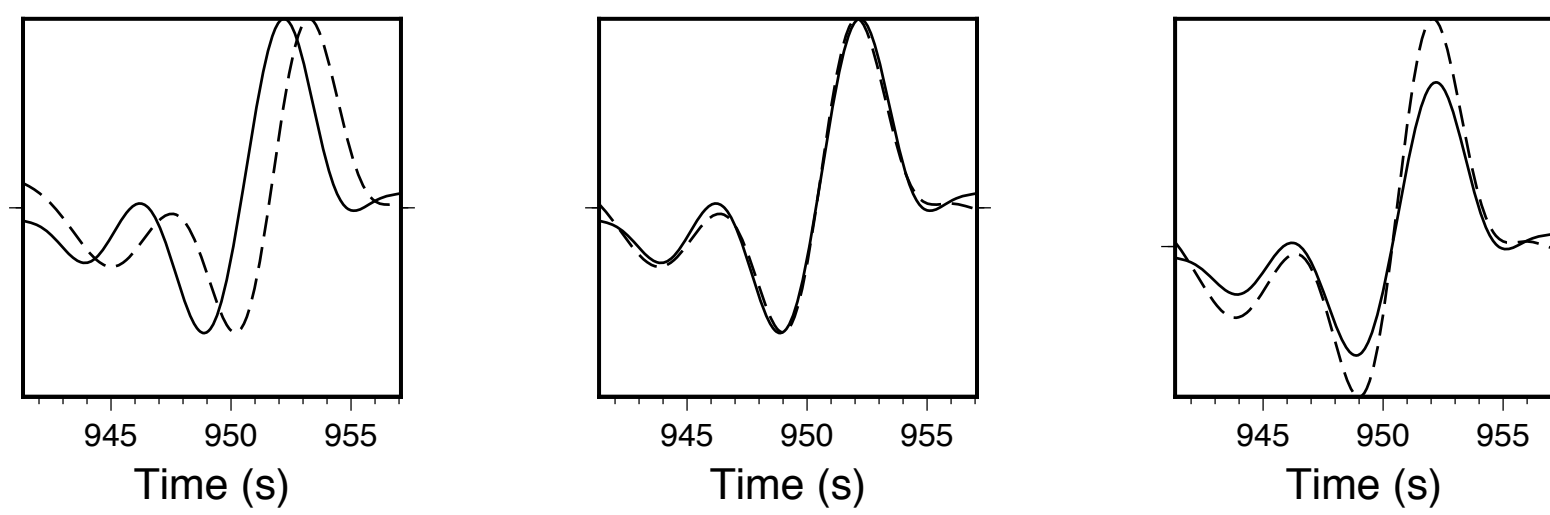
(a) Station: EDEY Event: lat=27.79° lon=86.04° depth=24.80km baz=28.33° Δ=101.63°



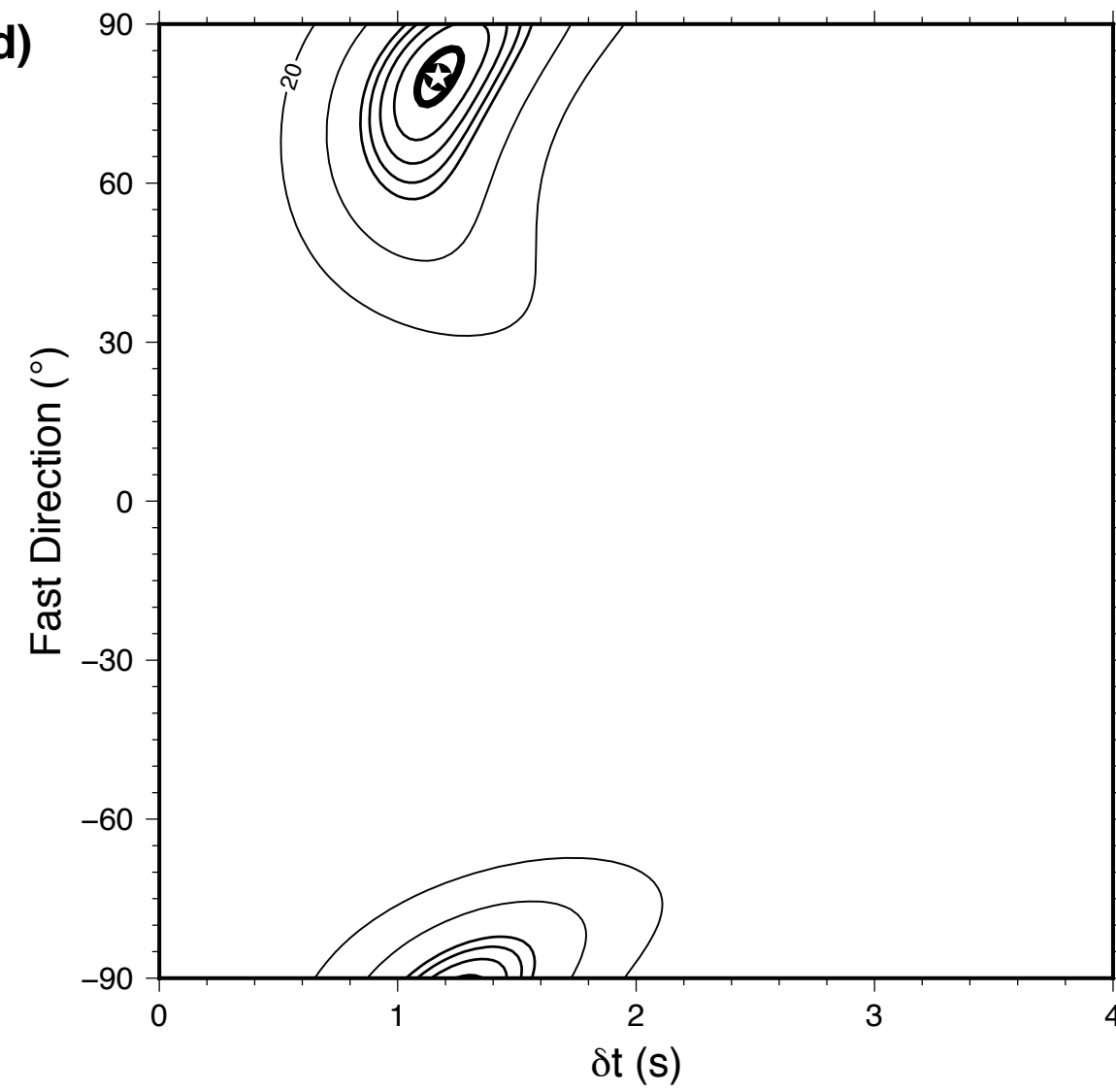
(b)



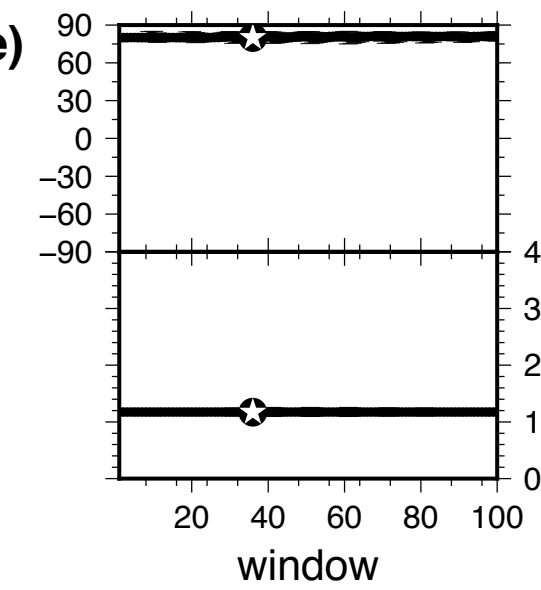
(c) Fast=80.00±2.75° δt=1.17±0.04(s)



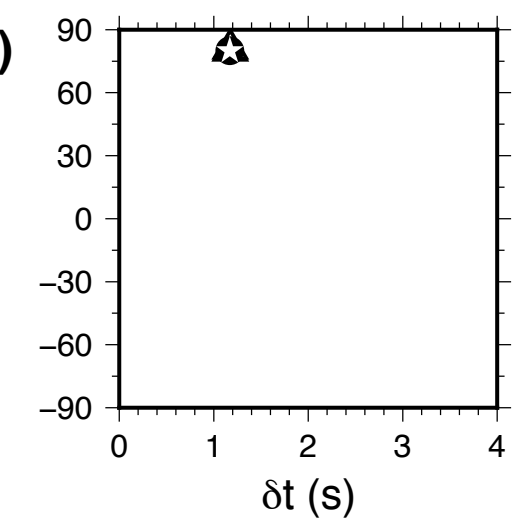
(d)



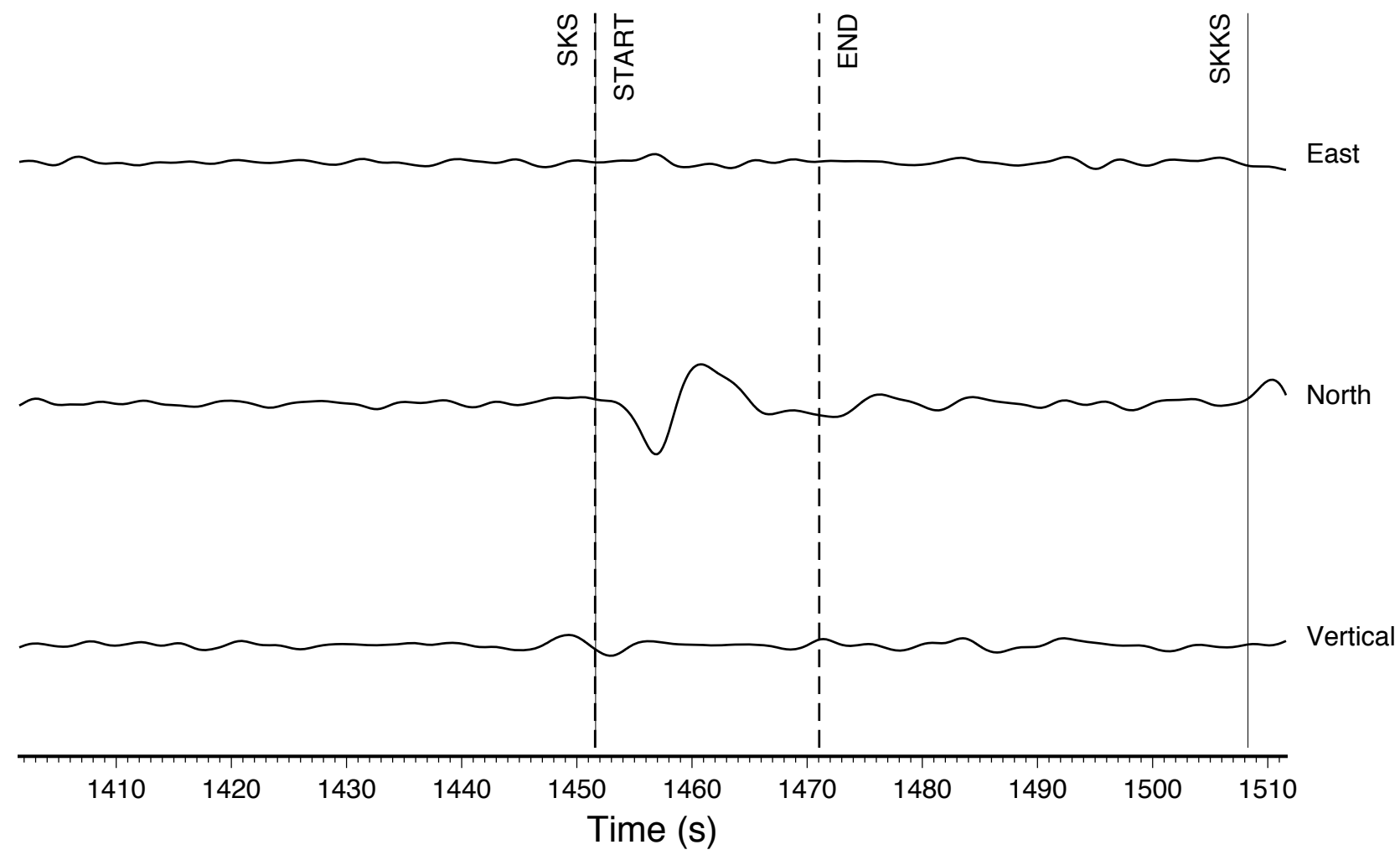
(e)



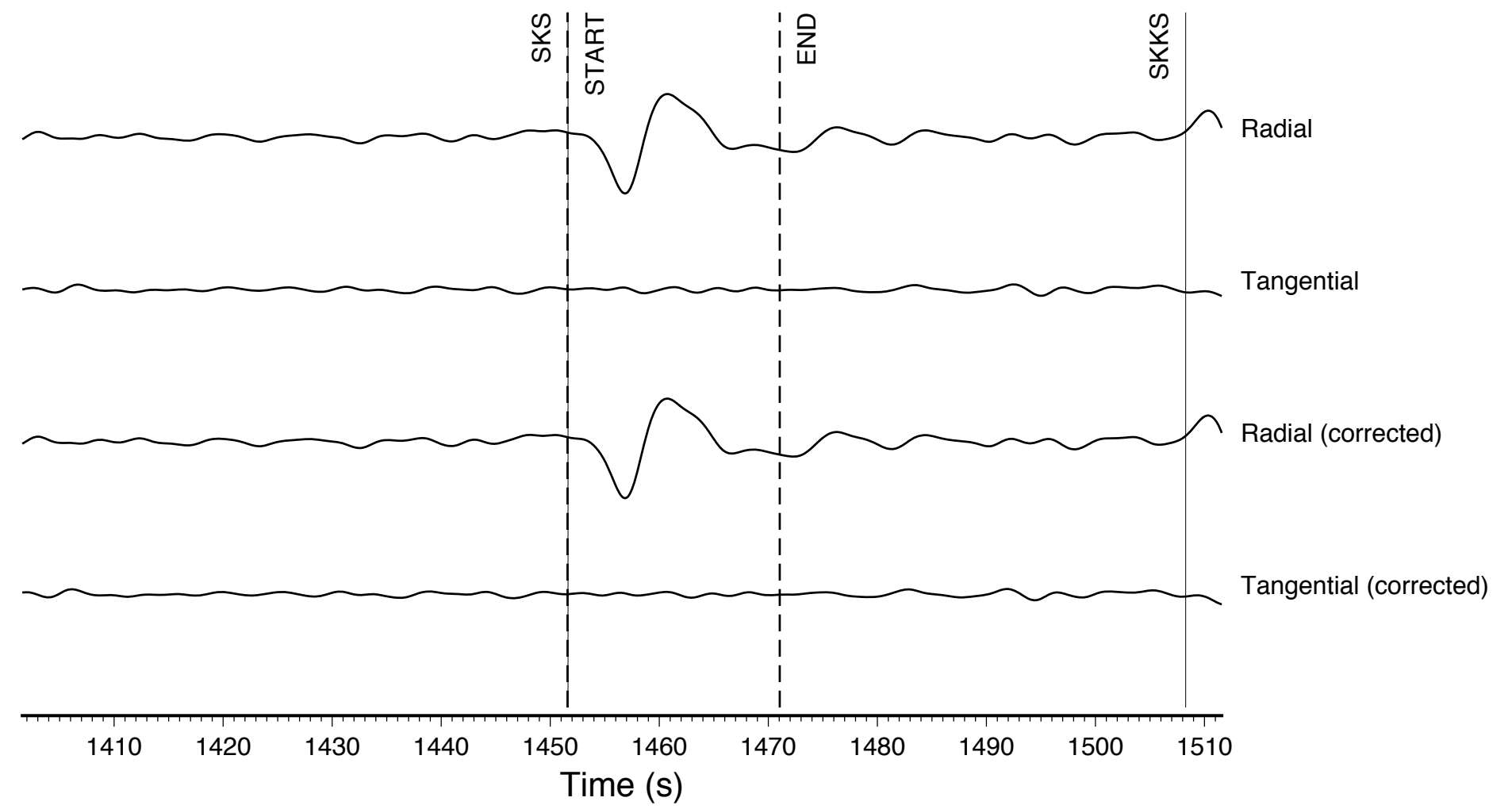
(f)



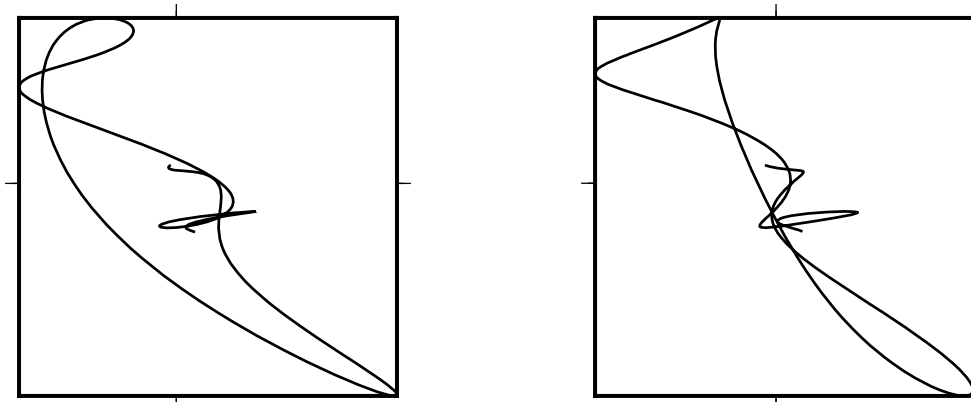
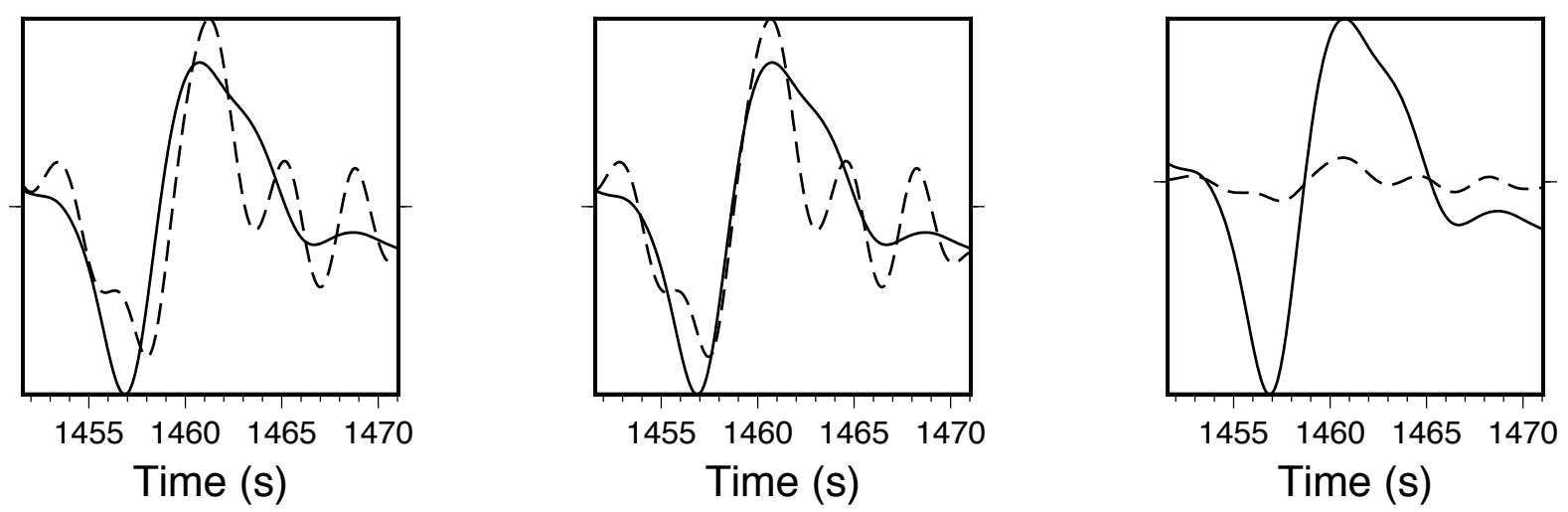
(a) Station: SJNN Event: lat=22.01° lon=142.71° depth=253.50km baz=344.88° Δ=109.35°



(b)

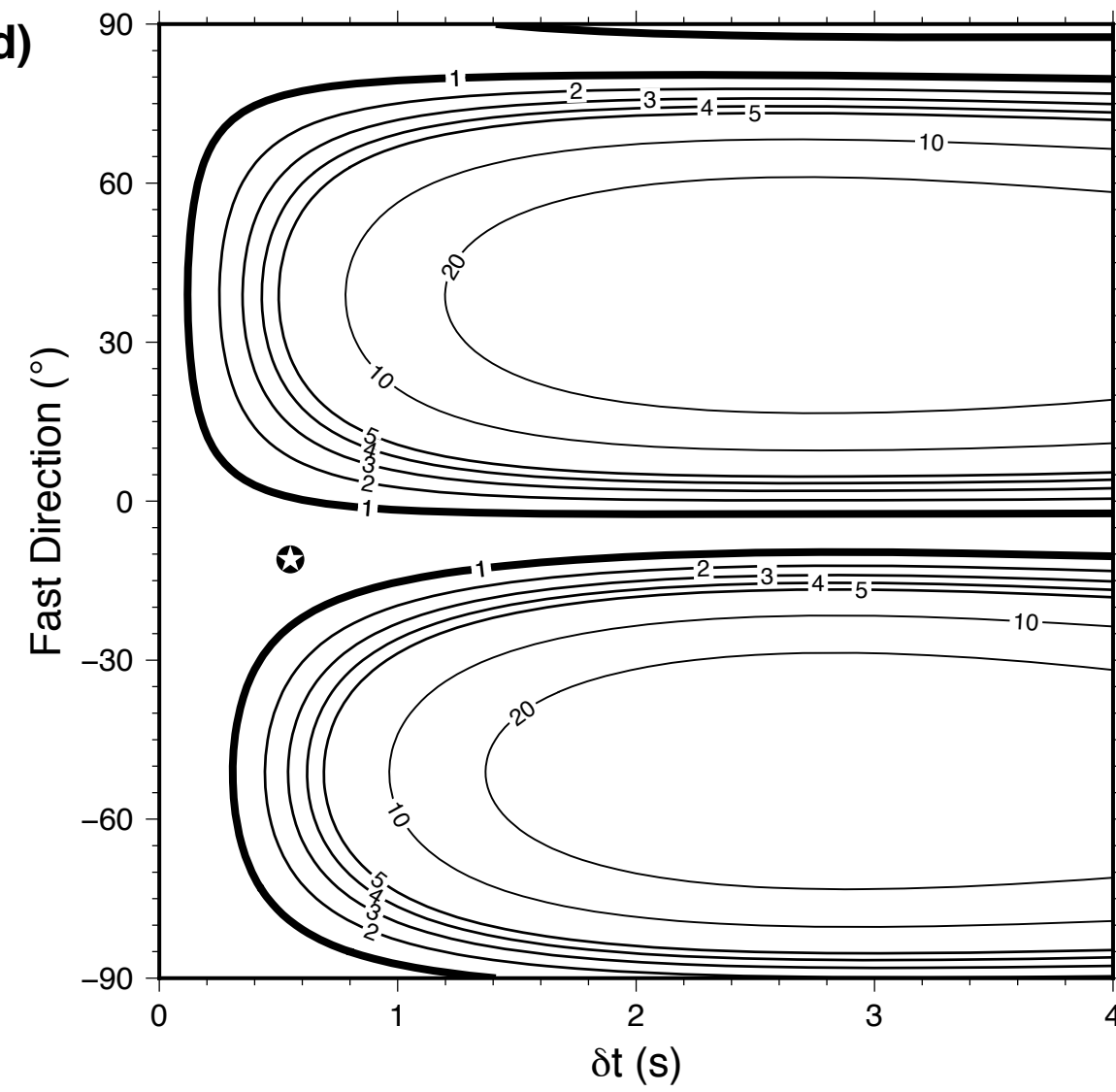


(c) Fast=-11.00±45.25° δt=0.55±1.00(s)

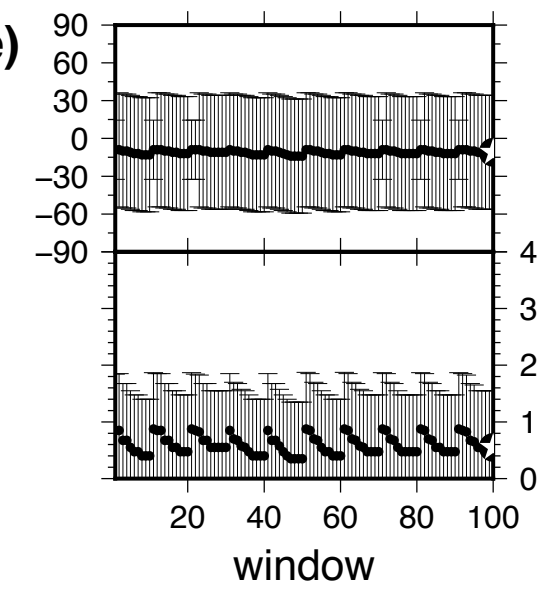


Particle motion

(d)



(e)



(f)

